IMPACT OF SOLAR RADIATION MODIFICATION ON TEMPERATURE CHANGES FROM SINABUNG ERUPTION IN KARO REGENCY

Sorja Koesuma[1,2*], Friska Ayu Sakhina[1], Rahmat Gernowo[3]

[1] *Departement of Physics, Faculty of Mathematics and Natural Science, Sebelas Maret University, Jl. Ir. Sutami 36A Kentingan Jebres, Surakarta, 57762, Indonesia*

[2]*Disaster Research Centre, Sebelas Maret University, Jl. Ir. Sutami 36A Kentingan Jebres, Surakarta, 57762, Indonesia*

[3]*Departement of Physics, Faculty of Science and Mathematics, Diponegoro University, Jl. Prof. Soedharto, SH, Tembalang, Semarang, 50275, Indonesia*

*email: sorja@staff.uns.ac.id

ABSTRACT

This study combines reanalysis of observational data and climate modelling to examine temperature changes due to the eruption of Mount Sinabung and future temperature projections. Observation data were taken from ERA5 to identify local temperature changes following the Sinabung eruption in February 2018, while simulations from the Geoengineering Model Intercomparison Project (GeoMIP) were used to observe temperature responses under the Solar Radiation Modification (SRM) scenario. Temperature projections were conducted for the period 2026 – 2099 using the CESM-WACCM, CNRM-ESM2-1, and MPI-ESM1-2-LR models under the G6Solar, G6Sulfur, SSP2-4.5, and SSP5-8.5 scenarios. The results show that GeoMIP temperatures are lower than ERA5 after bias correction. SRM was found to effectively decrease temperature at the summit of Sinabung and Karo Regency, approaching low emission scenarios (SSP2-4.5), with increases of 1,90℃ and 1,05℃ under G6Solar, and 1,02℃ and 0,96℃ under G6Sulfur. Conversely, in the high emission scenarios (SSP5-8.5), temperatures increased to 2,13℃ and 2,1℃.

Keywords: *Sinabung eruption; Solar Radiation Modification; ERA5; Temperature projection; Bias correction*

INTRODUCTION

Global surface temperatures in the last two decades have increased due to greenhouse gas emissions (IPCC, 2023). Extreme temperatures pose a significant threat to living things (Nogueira & Soares, 2019). The 2015 Paris Agreement, as an international policy focused on global warming, sets targets to keep "global average temperature rise well below 2°C compared to pre-industrial levels" and encourages efforts "to limit temperature rise to 1.5°C above pre-industrial levels" (Silvy et al., 2024). Indonesia, as a tropical island country, is vulnerable to the impacts of climate change. Supari et al., (2016), show the warming of surface temperatures over the past three decades throughout Indonesia, Putri & Suhadi, (2024) show the warming trend with an increase in the daytime minimum temperature trend and an increase in the night time minimum temperature trend.

In addition to mitigation, adaptation, and climate targets in the Paris Agreement, a variety of other alternatives have been put forward to address climate change, including climate interventions through climate interventions through geoengineering (Camilloni et al., 2022; Keith & MacMartin, 2015; MacCracken, 2009). One of the strategies of geoengineering was Solar Radiation Modification (SRM), which is a method of lowering the Earth's temperature by reducing or reflecting solar radiation (Kumler et al., 2025; Lawrence et al., 2018). Modelling studies that have been conducted to date show that SRM has the potential to provide a rapid drop in temperature, thus limiting the peak of global warming to 1.5°C (Irvine et al., 2019; Wieners et al., 2023).

One of the most studied methods of SRM, namely SAI, with a natural analogy of SAI, is such as the eruption of Mount Pinatubo in 1991, which injected 17 megatons of sulfur dioxide into the stratosphere, resulting in a global temperature drop of about 0.14 – 0.5°C for two years after the eruption (Kumler et al., 2025). Simulation solar geoengineering has been simulated in the Geoengineering Model Intercomparison Project (GeoMIP) (Kravitz et al., 2011, 2021).

Volcanic eruption activity can release significant amounts of SO2 gas into the atmosphere (Bluth et al., 1993; Kristiansen et al., 2024). Sulfur gas has a substantial climate impact, namely the reflection of incoming sunlight and a decrease in temperature on the Earth's surface through the formation of acidic aerosols in the atmosphere (Robock, 2000; Staunton-Sykes et al., 2021). Indonesia has many active volcanoes, and one of the

most active volcanoes is the Sinabung volcano in the highlands of Karo Regency, North Sumatra (Hanif et al., 2024). Based on SO_2 emissions, the Sinabung eruption was among the three most active volcanoes emitting gas in Indonesia during the period 2010–2019 (Bani et al., 2022; Kunrat et al., 2022).The Sinabung eruption on February 19, 2018, produced an ash column of 16.8 km and a SO2 column of up to 50 DU. In CALIPSO measurements, the presence of attenuation due to ash or aerosol is observed at an altitude of approximately 15–18 km (Hedelt et al., 2019). Karo Regency, North Sumatra, is situated in a highland area adjacent to Mount Sinabung and is highly vulnerable to future climate change (Pepin et al., 2022). Karo Regency is a major potato-producing area, so farmers face climate change risks, including frost, drought, and changes in weather patterns (Hasanah et al., 2025). Rising air temperatures affect changes in morphology and tuber development in potato plants (Handayani et al., 2013)and decrease potato crop production (Salwati et al., 2013). Therefore, the selection of the area of Karo Regency, North Sumatra as the focus of research is not only because of its volcanic activity, but also the increase in temperature that affects the agricultural sector, especially on potato production and the community, so it is important to observe and simulate climate change and SRM mitigation technology.

Based on the background that has been explained, research on the impact of the Sinabung eruption on local temperatures in Karo Regency remains limited, despite the area being directly affected by the eruption. This study aims to fill the gap by examining the temperature changes resulting from the Mount Sinabung eruption and comparing them with changes from the SRM scenario using GeoMIP simulations. Projections of future temperature changes through GeoMIP simulations are also carried out to see how temperature increases can be limited through SRM scenarios that can later affect the agricultural sector and society, as well as a reference for facing global warming.

METHODS

Study Area

Mount Sinabung in Karo Regency, North Sumatra, with an altitude of 2,460 m above sea level and coordinates 98° 23'32.98" E, 3° 10'14.54" N, is the most active volcano in Indonesia (Hanif & Apichontrakul, 2023). The Sinabung eruption on February 19, 2018, at approximately 02:55 UTC became one of the significant eruptions, producing a 16.8 km ash column and a SO2 column of up to 50 DU, as observed through several satellites, including TROPOMI, OMI, IASI, MLS, and CALIPSO/CALIOP. In CALIPSO measurements, attenuation due to ash or aerosol is observed at an altitude of approximately 15–18 km. The Center for Volcanology and Geological Disaster Mitigation (PVMBG) also reported dark gray ash columns with large volumes rising up to 16.8 km (Hedelt et al., 2019). The focus of the research is in Karo Regency, North Sumatra which is at the coordinates of 2.833° - 3.317° N, 97.917° - 98.633° E and the map displayed is in a wider area to see the temperature change more clearly which is 2.5° – 4° N and 97.5° – 99.5° E as Figure 1.

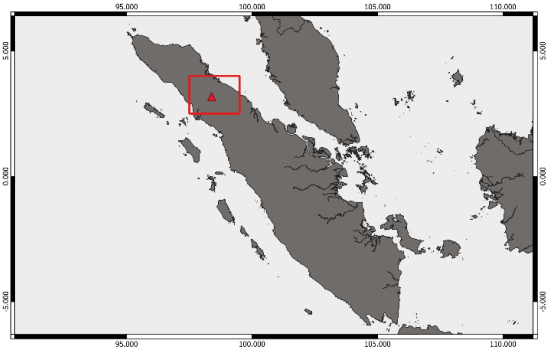

Figure 1. Study Area

Climate Data

Secondary temperature data were obtained from ECMWF (European Centre for Medium-Range Weather Forecasts) Reanalysis v5 or ERA5 reanalysis by C3S (Copernicus Climate Change Service), which serves as observational data based on reanalysis. ERA5 data were used for the t2m variable, with a baseline range of 1990–2014 and February 2018 as the incidence data.

Simulations of SRM were carried out through the GeoMIP (Geoengineering Model Intercomparison Project) model through several models, including CESM2-WACCM which has 228 chemical types to represent chemical processes across the atmosphere layer and can predict the formation of stratosphere aerosols, CNRM-ESM2-1 which is designed to study chemical processes, aerosols, and carbon feedback in projections, and MPI-ESM1-2-LR which works by forcing the distribution of sulfate aerosols calculated using MAECHAM5-HAM model. And, four scenarios are used, such as G6Solar with an ideal reduction of the solar constant, G6sulfur with SO2 injection which will later form sulfate aerosols into the stratosphere (Jones et al., 2021), SSP2-4.5 with a radiation forcing rate of 4.5 W/m2 (Deng et al., 2023) in 2100 and SSP5-8.5 with a radiative forcing rate of 8.5 W/m2 (Khardekar et al., 2025). The GeoMIP model used is presented in Table 1.

Table 1. Simulation of the model from GeoMIP used in the study

Model Name	Variant	Resolution *	Period	Source
CESM-WACCM	r1i2p1f1	288 × 192	2015 – 2100	(Danabasoglu, 2019)
CNRM-ESM2-1	r1i1p1f2	256 × 128	2015 – 2100	(Seferian, 2023)
MPI-ESM1-2-LR	r1i1p1f1 r2i1p1f1 r3i1p1f1	192 x 96	2015 – 2100	(Niemeier *et al.*, 2019)

*Resolution in grid points at horizontal latitude × longitude by (Piani, Haerter, et al., 2010).

Processing Data

To improve the surface temperature accuracy of the model on climate projections, bias correction was performed to eliminate bias between the model and the observation (Minville et al., 2008), and the projection temperature was consistent with historical observation data (Narenpitak et al., 2024). The method employed combines two approaches: linear regression and distribution transformation. In the initial stage, linear regression was carried out without interception between the model data (Xmod) and the observation data (Yobs) (Gudmundsson et al., 2012):

$$f(x) = bx \quad (1)$$

$$f(x) = a + b \times x \quad (2)$$

$$Yobs = a + b \times Xmod \quad (3)$$

With Yobs is observation, Xmod is the model, a is the intercept, and b is the slope. The regression results are then used to transform the model distribution to resemble the observation distribution. This process follows the cumulative distribution equalization as follows (Piani, Weedon, et al., 2010):

$$CDFobs(f(x)) = CDFmod(x) \quad (4)$$

The transformation was carried out using the Gaussian CDF (Cumulative Distribution Function) approach, then adjusted using a first-order polynomial model.

From the bias correction, a comparison was made between the GeoMIP model data and the ERA5 observation data for the period 1990–2014. Then, the results are applied to future temperature projections from future GeoMIP data from the G6Solar, G6Sulfur, SSP2-4.5, and SSP5-8.5 scenarios. The projections are divided into four 25-year periods, allowing for more detailed analysis based on time trends. All results of bias correction data are stored in NetCDF format.

RESULT AND DISCUSSION

Analysis of Temperature Changes in the Eruption of Mount Sinabung

The eruption of Mount Sinabung in Karo Regency occurred on February 19, 2018. In Figure 2, the scattering of ash during the eruption is captured by the MODIS satellite. The Center for Volcanology and Geological Disaster Mitigation (PVMBG) explained that the distribution of volcanic ash was heading south to southwest and reported ash columns with large volumes rising to 16.8 km. The grayish-brown color indicates solid volcanic materials, such as dust, volcanic ash, and sulfur gas. The hot cloud of avalanches moved up to 4.9 km to the south–southeast and 3.5 km to the east–southeast.

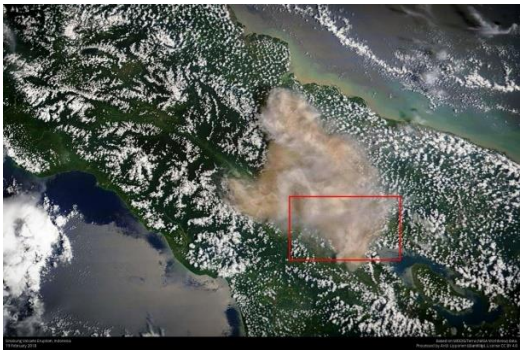

Figure 2. Sinabung eruption on February 19, 2018, from the MODIS satellite (NASA, 2018)

Figure 3, it is found that the temperature in Karo Regency on February 19 decreased until the 23rd, on February 20 the temperature decrease extended to the southwest and south, on February 21 it expanded to the northwest and south, on the 22nd it extended to the southeast, and on February 23 became the peak of the temperature decrease.

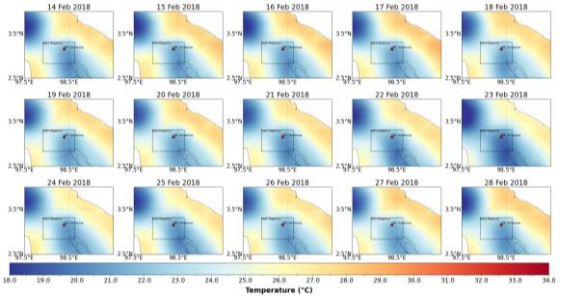

Figure 3. Temperature 14 February – 28 February 2018 (ERA5)

The eruption event is marked with an arrow on the graph, indicating temperatures of 22.2°C at the top of Mount Sinabung and 22.9°C in

Karo Regency (Figure 4). At the top of Sinabung, the highest temperature occurred on February 18 at 22.5°C, then decreased during the eruption on February 19 to 22.2°C because volcanic ash from the eruption blocked solar radiation from entering, but again increased by 0.1°C on February 20 as volcanic ash spread and tended to fall to the plains around Mount Sinabung. Temperatures began to drop back down or lower than before the eruption from February 21 to February 26, with a peak decline on February 23. This is because volcanic ash and SO_2, with a lifespan of 1–3 days, began to oxidize to H_2SO_4 in the stratosphere.

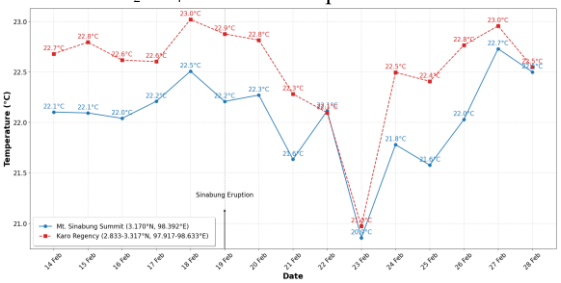

Figure 4. Temperature timeseries 14 February – 28 February 2018

The temperature in Karo Regency has decreased significantly from when the eruption occurred. This occurs because the Karo Regency area receives an equal distribution of ash and aerosols, as reported by PVMBG, in the direction of distribution, namely from south to southwest. Then, at the peak of Sinabung and Karo Regency, the temperature began to return to close to the values before the eruption around February 27-28, or about eight to nine days after the eruption. This suggests that the effects of the temperature drop due to eruptions are only temporary and will begin to disappear as ash and aerosols are spread more widely and thinly in the atmosphere.

Temperature Change Analysis from the GeoMIP Model

(a)

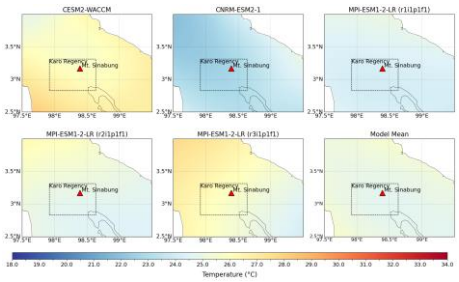

(b)

(c)

(d)

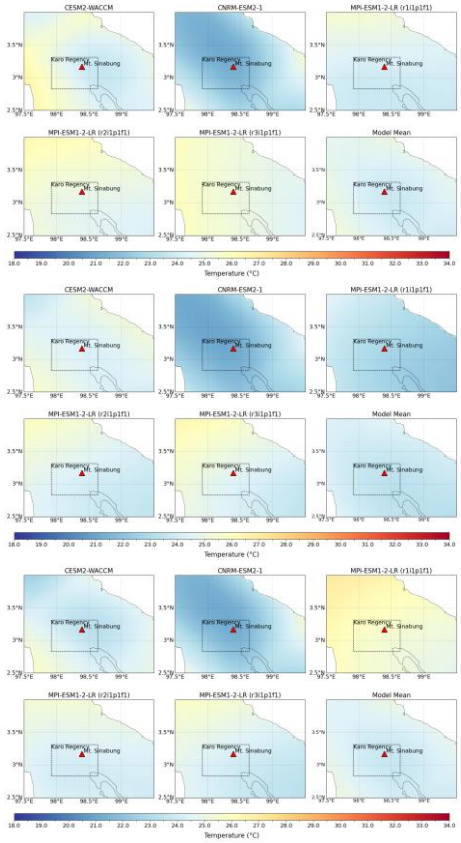

Figure 5. Temperature change on February 19, 2018, at the peak of Sinabung (a) G6Solar, (b) G6Sulfur, (c) SSP2-4.5, (d) SSP5-8.5

GeoMIP model data has a rougher spatial resolution than observation data, so the topography of areas such as mountains cannot be identified in the visualization of temperature during the eruption of Mount Sinabung. As in Figure 5, the area of Karo Regency that includes Mount Sinabung is seen to have a subtle gradation of temperature change and does not show temperature changes that follow the actual topographic contours. As a result, the resulting surface temperature tends to be the average value of the grid area and does not account for specific elevation differences.

The eruption of Mount Sinabung in February 2018 demonstrated how the injection of SO_2 into the atmosphere can reduce rapid local temperature decrease through the formation of sulfate aerosols, which increase atmospheric reflectivity and reduce incoming solar radiation. This mechanism forms the basis of the Solar Radiation Modification (SRM) scenario examined in this study, although SRM differs in that it is a deliberate, sustained intervention involving periodic SO_2 injections to achieve long-term, large-scale temperature decrease. As volcanic eruptions are unpredictable and impractical for climate mitigation, SRM is considered a controlled alternative. Accordingly, this study projects

temperature changes in Karo Regency, North Sumatra, for the period 2026 – 2099 using SRM simulations for the GeoMIP.

Analysis of Projected Temperature Change with Solar Radiation Modification (SRM) in 2026 – 2099

1. G6Solar

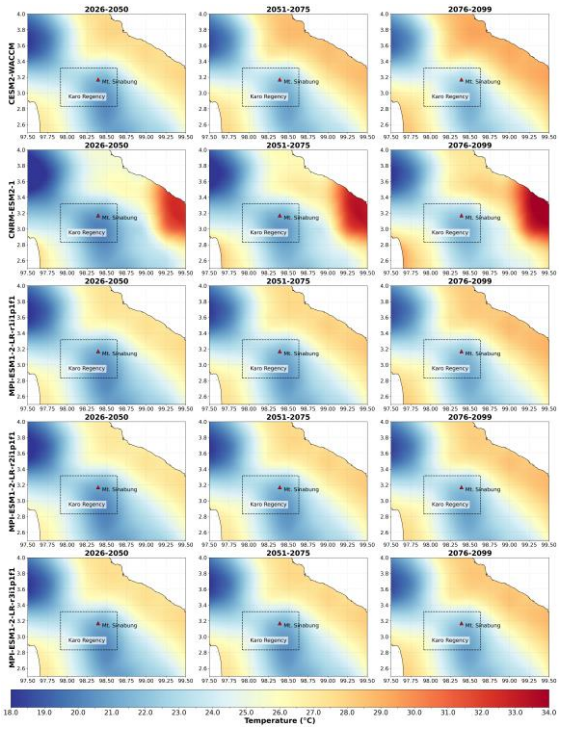

Figure 6. Temperature projections of 2026 – 2099 in the G6Solar scenario

In general, the temperature in each model shows a consistent increase throughout the 21st century (Figure 6). At the beginning of the period, specifically from 2026 to 2050, the average annual temperature ranges from 21°C to approximately 23°C. However, towards the end of the period, specifically the 2090s, the temperature increased in the range of 22°C to nearly 24°C. Then, in Karo Regency at the beginning of the period, namely 2026 – 2050, the annual average temperature was in the range of 21 to close to 23°C, and towards the end of the period, namely in the 2090s, the temperature increased to 24°C.

2. G6Sulfur

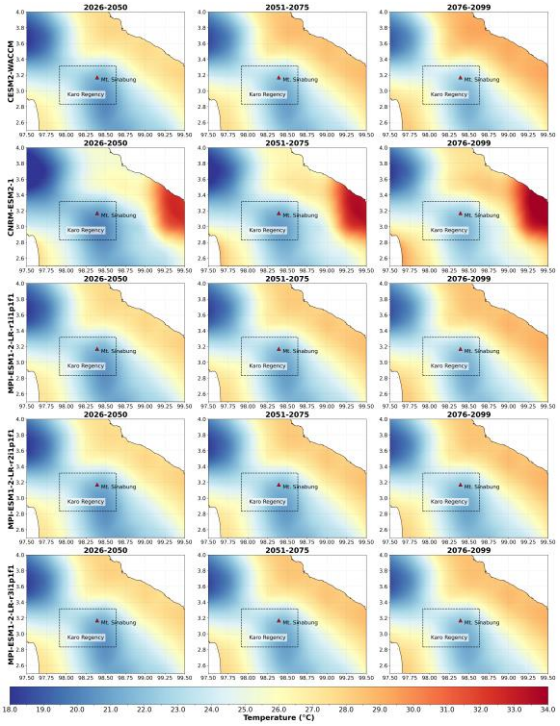

Figure 7. Projected temperature of 2026 – 2099 in the G6Sulfur scenario

Each model shows a consistent increase in temperature throughout the 21st century (Figure 7). At the beginning of the period, specifically from 2026 to 2050, the annual average temperature at the summit of Mount Sinabung ranges from 21°C to 23°C. However, towards the end of the period, specifically the 2090s, the temperature increased in the range of 22°C to nearly 24°C. Then, in Karo Regency, the initial temperature of the period was in the range of 21 – 23°C, and towards the end of the period, the temperature increased to 24°C.

3. SSP2-4.5

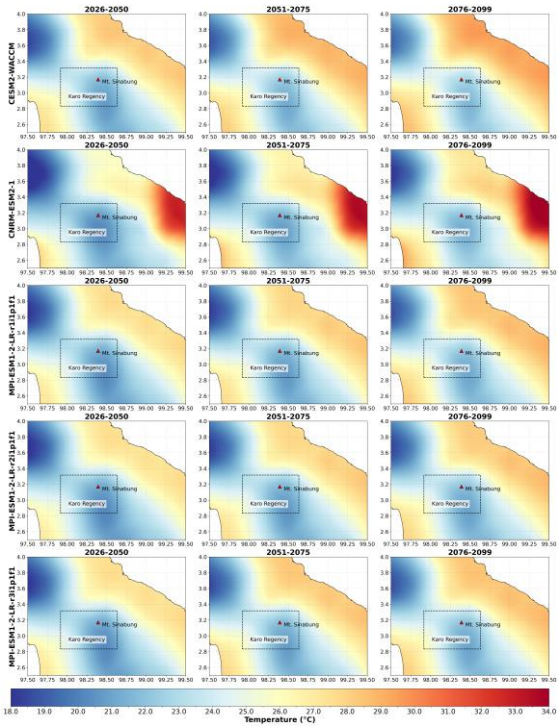

Figure 8. Projected temperature 2026 – 2099 in the SSP2-4.5 scenario

Each model shows a consistent increase in temperature throughout the 21st century (Figure 8). At the beginning of the period, specifically from 2026 to 2050, the annual average temperature at the summit of Mount Sinabung was between 21 °C and 23°C. Towards the end of the period, specifically the 2090s, the temperature increased to nearly 24°C. Then, in Karo Regency at the beginning of the period, the average annual temperature was at 21-23°C, and at the end of the period, the temperature increased to 24°C.

4. SSP5-8.5

In the SSP5-8.5 scenario, the temperature change is significantly higher than in other scenarios, especially the G6Solar and G6Sulfur scenarios. This is because SSP5-8.5 is a high-level emission scenario with a radiation forcing of 8.5 W/m², while the G6Solar and G6Sulfur scenarios involve SRM to compensate for the warming resulting from SSP5-8.5. So, from the results obtained with the G6Solar and G6Sulfur scenarios, it can compensate by slightly holding the heating rate compared to the absence of SRM scenarios with high emission levels, such as SSP5-8.5.

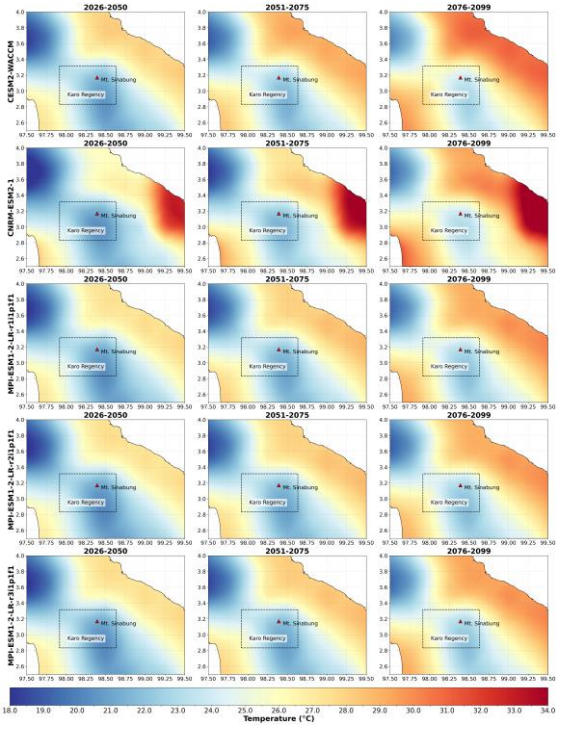

Figure 9. Projected temperature 2026 – 2099 in the SSP5-8.5 scenario

Each model shows a consistent increase in temperature throughout the 21st century (Figure 9). The graph results of this SSP5-8.5 scenario also show a sharp increase between years. At the beginning of the period, specifically from 2026 to 2050, the average annual temperature at the summit of Mount Sinabung was 22–23°C. Towards the end of the period, namely the 2090s, the temperature increased to 23-26°C. Then, in Karo Regency, at the beginning of the period, the temperature was 22–23°C, and towards the end of the period, it increased sharply to 23–26°C.

5. Average projections

Figure 10 illustrates the temperature change from 1990 to 2099, with the period from 1990 to 2024 representing observational data and the period from 2026 to 2099 representing projections from GeoMIP. From observations to GeoMIP, it decreased at the beginning of the year, specifically in 2026, and then increased significantly until 2099. From the results of each scenario, it can be seen that in the G6Solar and G6Sulfur scenarios, it can limit the temperature rise below SSP5-8.5 and almost close to SSP2-4.5

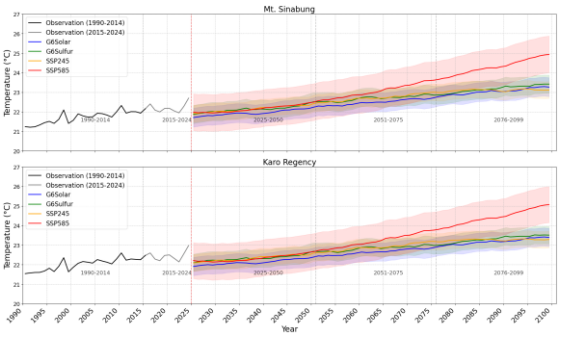

Figure 10. Temperature projection chart for 2026 – 2099

The G6Sulfur scenario represents SO2 injection and illustrates how an eruption that injects SO2 affects the temperature, as seen in the Sinabung eruption, which is projected to continue until 2099. This is also in line with how the Sinabung eruption can lower the temperature, as shown in the timeseries graph in Figure 4. The similarity of principles between G6Sulfur and the impact of the Sinabung eruption strengthens the understanding that sulfur injection, both natural and artificial, can have a significant effect on surface temperature. However, the impact of the temperature drop from the eruption is only temporary, and with a drastic downward spike, in contrast to the SRM scenario, which can run over a long period of time, and the decline occurs gradually.

Table 2. Temperature history and projections from 1990 to 2099

Peak of Mount Sinabung (°C)			
History	**1990 - 2014**	**2015 - 2024**	**1990 - 2024**
ERA5	21,71	22,20	21,85
Skenario	**2025 - 2050**	**2051 - 2075**	**2075 - 2099**
G6Solar	21,96	22,48	23,05
G6Sulfur	22,15	22,70	23,17
SSP2-4.5	22,15	22,71	23,11
SSP5-8.5	22,16	23,06	24,29
Kabupaten Karo (°C)			
History	**1990 - 2014**	**2015 - 2024**	**1990 - 2024**
ERA5	22,01	22,45	22,13
Skenario	**2025 - 2050**	**2051 - 2075**	**2075 - 2099**
G6Solar	22,13	22,64	23,18
G6Sulfur	22,34	22,84	23,30
SSP2-4.5	22,34	22,89	23,27
SSP5-8.5	22,33	23,22	24,43

From Table 2, it can be seen that the total temperature change is from 1990 to 2099. G6Solar represents SRM intervention by reducing incoming solar radiation. The total temperature increase from 1990 to 2099 was 1.2°C at the peak of Sinabung and 1.18°C in Karo Regency. Additionally, the total projected increase from 2055 to 2099 is 1.09°C at the peak of Sinabung and 1.05°C in Karo Regency.

In the G6Sulfur scenario, involving the injection of sulfur into the stratosphere as a form of SRM. The total temperature increase from 1990 to 2099 was 1.46°C at the peak of Sinabung and 1.29°C in Karo Regency. Additionally, the total projected increase from 2055 to 2099 is 1.02°C at the peak of Sinabung and 0.96°C in Karo Regency.

The SSP2-4.5 scenario illustrates a low-level emission pathway without SRM intervention and moderate climate adaptation. The temperature at the end of the century of this scenario is almost equivalent to that of G6Solar and G6Sulfur, suggesting that *geoengineering strategies* can mimic the effects of moderate emissions on SSP2-4.5, albeit with a very different approach. The total temperature increase from 1990 to 2099 was 1.4°C at the peak of Sinabung and 1.26°C in Karo Regency. Additionally, the total projected increase from 2055 to 2099 is 0.96°C at the peak of Sinabung and 0.93°C in Karo Regency.

The SSP5-8.5 scenario represents a high-level emission path with minimal SRM intervention and adaptation. This scenario exhibits the sharpest warming trend among all other scenarios. In addition, this scenario resulted in a total temperature increase from 1990 to 2099, with peaks of 2.58°C at Sinabung and 2.42°C in Karo Regency. Additionally, the total projected increase from 2055 to 2099 is 2.13°C at the peak of Sinabung and 2.1°C in Karo Regency.

From the results of the projections of the four scenarios, it is known that the G6Solar and G6Sulfur scenarios are able to limit global warming significantly from SSP5-8.5 and are almost close to SSP2-4.5. This is as explained B. Kravitz *et al.*, (2015), the purpose of the experiment using the G6Solar and G6Sulfur scenarios was to modify the simulation based on the scenario with the highest coercion, i.e., SSP5-8.5, and to follow the evolution of the intermediate coercion scenario SSP2-4.5.

Although SRM can reduce the rate of warming, as in the G6Solar and G6Sulfur scenarios, SRM can only address incoming symptoms or incoming energy, not address the direct cause, namely, greenhouse gas emissions, such as CO2. If the intervention from SRM is stopped suddenly, extreme and rapid temperature spikes can occur. And, this SRM must be done in the long term.

CONCLUSION

According to this study, the Sinabung eruption on February 19, 2018, was found to lower the temperature within a few days. This happened because the eruption produced many materials, one of which was SO2, which could reduce the temperature. The analogy of this eruption is similar to how the SRM scenario works, namely, G6Sulfur. In this study, the temperature projections for 2026–2099 scenarios G6Solar and G6Sulfur successfully

limited the temperature rise to close to SSP2-4.5 and below SSP5-8.5. The temperature increase in 2026 – 2099 for the G6Solar scenario at the peak of Sinabung is 1.09°C and in Karo Regency is 1.05°C, the G6Sulfur scenario at the peak of Sinabung is 1.02°C and in Karo Regency is 0.96°C, the SSP2-4.5 scenario at the peak of Sinabung is 0.96°C and in Karo Regency is 0.93°C, and the SSP5-8.5 scenario at the peak of Sinabung is 2.13°C and in Karo Regency is 2.1°C.

Based on the research conducted, the recommendation for further research is to incorporate sulfur dioxide data into the projections, enabling the determination of the amount of SO2 injection required to achieve the temperature reduction target. This should be linked to the effects of rainfall and air humidity resulting from the temperature reduction caused by the Sinabung Eruption.

RERERENCES

Bani, P., Oppenheimer, C., Tsanev, V., Scaillet, B., Primulyana, S., Saing, U. B., Alfianti, H., & Marlia, M. (2022). Modest volcanic SO2 emissions from the Indonesian archipelago. *Nature Communications*, *13*(1), 3366.

Bluth, G. J. S., Schnetzler, C. C., Krueger, A. J., & Walter, L. S. (1993). The contribution of explosive volcanism to global atmospheric sulphur dioxide concentration. *Nature*, *366*, 327–329.

Camilloni, I., Montroull, N., Gulizia, C., & Saurral, R. I. (2022). La Plata Basin hydroclimate response to solar radiation modification with Stratospheric Aerosol Injection. *Frontiers in Climate*, *4*, 1–11.

Danabasoglu, G. (2019). *NCAR CESM2-WACCM model output prepared for CMIP6 GeoMIP G6solar*. Earth System Grid Federation.

Deng, Z., Javanroodi, K., Nik, V. M., & Chen, Y. (2023). Using urban building energy modeling to quantify the energy performance of residential buildings under climate change. *Building Simulation*, *16*(9), 1629–1643.

Gudmundsson, L., Bremnes, J. B., Haugen, J. E., & Engen-Skaugen, T. (2012). Technical Note: Downscaling RCM precipitation to the station scale using statistical transformations – A comparison of methods. *Hydrology and Earth System Sciences*, *16*(9), 3383–3390.

Handayani, T., Basunanda, P., Murti, R., & dan Sofiari, E. (2013). Perubahan Morfologi dan Toleransi Tanaman Kentang Terhadap Suhu Tinggi. *J. Hort*, *23*(4), 318–328.

Hanif, M., & Apichontrakul, S. (2023). Vertical Ground Deformation Monitoring of the Sinabung Volcano in 2021-2022 using Sentinel-1 and DInSAR. *12th International Conference on Environmental Engineering, Science and Management*.

Hanif, M., Apichontrakul, S., & Razi, P. (2024). Surface deformation monitoring and forecasting of sinabung volcano using interferometry synthetic aperture radar and forest-based algorithm. *Remote Sensing Applications: Society and Environment*, *36*, 1–15.

Hasanah, K., Brotodjojo, R. R. R., & Poerwanto, M. E. (2025). Enhancing government communication for climate change adaptation : a case study of agricultural policies and practices. *Interaksi: Jurnal Ilmu Komunikasi*, *14*(1), 222–239.

Hedelt, P., Efremenko, D. S., Loyola, D. G., Spurr, R., & Clarisse, L. (2019). Sulfur dioxide layer height retrieval from Sentinel-5 Precursor/TROPOMI using FP_ILM. *Atmospheric Measurement Techniques*, *12*, 5503–5517.

IPCC. (2023). *IPCC Sixth Assessment Report (Ar6) "Climate Change 2023."* 1–85.

Irvine, P., Emanuel, K., He, J., Horowitz, L. W., Vecchi, G., & Keith, D. (2019). Halving warming with idealized solar geoengineering moderates key climate hazards. *Nature Climate Change*, *9*(4), 295–299.

Jones, A., Haywood, J. M., Jones, A. C., Tilmes, S., Kravitz, B., & Robock, A. (2021). North Atlantic Oscillation response in GeoMIP experiments G6solar and G6sulfur: Why detailed modelling is needed for understanding regional implications of solar radiation management. *Atmospheric Chemistry and Physics*, *21*(2), 1287–1304.

Keith, D. W., & MacMartin, D. G. (2015). A temporary, moderate and responsive scenario for solar geoengineering. *Nature Climate Change*, *5*, 201–206.

Khardekar, P., Bhawar, R. L., Kumar, V., & Chaudhari, H. S. (2025). Future Projections of Clouds and Precipitation Patterns in South Asia: Insights from CMIP6 Multi-Model Ensemble Under SSP5 Scenarios. *Climate*, *13*(2).

Kravitz, B., MacMartin, D. G., Visioni, D., Boucher, O., Cole, J. N. S., Haywood, J., Jones, A., Lurton, T., Nabat, P., Niemeier, U., Robock, A., Séférian, R., & Tilmes, S. (2021). Comparing different generations of idealized solar geoengineering simulations in the Geoengineering Model Intercomparison

Project (GeoMIP). *Atmospheric Chemistry and Physics*, *21*(6), 4231–4247.

Kravitz, B., Robock, A., Boucher, O., Schmidt, H., Taylor, K. E., Stenchikov, G., & Schulz, M. (2011). The Geoengineering Model Intercomparison Project (GeoMIP). *Atmospheric Science Letters*, *12*, 162–167.

Kravitz, B., Robock, A., Tilmes, S., Boucher, O., English, J. M., Irvine, P. J., Jones, A., Lawrence, M. G., MacCracken, M., Muri, H., Moore, J. C., Niemeier, U., Phipps, S. J., Sillmann, J., Storelvmo, T., Wang, H., & Watanabe, S. (2015). The Geoengineering Model Intercomparison Project Phase 6 (GeoMIP6): Simulation design and preliminary results. *Geoscientific Model Development*, *8*, 3379–3392.

Kristiansen, N. I., Witham, C. S., & Beckett, F. M. (2024). A modelling approach for quantifying volcanic sulphur dioxide concentrations at flight altitudes and the potential hazard to aircraft occupants. *Journal of Applied Volcanology*, *13*, 1–14.

Kumler, A., Kravitz, B., Draxl, C., Vimmerstedt, L., Benton, B., Lundquist, J. K., Martin, M., Jean, H., Wang, H., Lennard, C., & Tao, L. (2025). Potential effects of climate change and solar radiation modification on renewable energy resources. *Renewable and Sustainable Energy Reviews*, *207*, 1–14.

Kunrat, S., Kern, C., Alfianti, H., & Lerner, A. H. (2022). Forecasting explosions at Sinabung Volcano, Indonesia, based on SO2 emission rates. *Frontiers in Earth Science*, *10*, 1–15.

Lawrence, M. G., Schäfer, S., Muri, H., Scott, V., Oschlies, A., Vaughan, N. E., Boucher, O., Schmidt, H., Haywood, J., & Scheffran, J. (2018). Evaluating climate geoengineering proposals in the context of the Paris Agreement temperature goals. *Nature Communications*, *9*(1), 3734.

MacCracken, M. C. (2009). On the possible use of geoengineering to moderate specific climate change impacts. *Environmental Research Letters*, *4*.

Minville, M., Brissette, F., & Leconte, R. (2008). Uncertainty of the impact of climate change on the hydrology of a nordic watershed. *Journal of Hydrology*, *358*, 70–83.

Narenpitak, P., Kongkulsiri, S., Tomkratoke, S., & Sirisup, S. (2024). Regional impacts of solar radiation modification on surface temperature and precipitation in Mainland Southeast Asia and the adjacent oceans. *Scientific Reports*, *14*(1), 22713.

Niemeier, U., Wieners, K.-H., Giorgetta, M., Jungclaus, J., Reick, C., Esch, M., Bittner, M., Legutke, S., Schupfner, M., Wachsmann, F., Gayler, V., Haak, H., de Vrese, P., Raddatz, T., Mauritsen, T., von Storch, J.-S., Behrens, J., Brovkin, V., Claussen, M., … Roeckner, E. (2019). *MPI-M MPI-ESM1.2-LR model output prepared for CMIP6 GeoMIP G6solar*. Earth System Grid Federation.

Nogueira, M., & Soares, P. M. M. (2019). A surface modelling approach for attribution and disentanglement of the effects of global warming from urbanization in temperature extremes: Application to Lisbon. *Environmental Research Letters*, *14*, 1–10.

Pepin, N. C., Arnone, E., Gobiet, A., Haslinger, K., Kotlarski, S., Notarnicola, C., Palazzi, E., Seibert, P., Serafin, S., Schöner, W., Terzago, S., Thornton, J. M., Vuille, M., & Adler, C. (2022). Climate Changes and Their Elevational Patterns in the Mountains of the World. *Reviews of Geophysics*, *60*(1).

Piani, C., Haerter, J. O., & Coppola, E. (2010). Statistical bias correction for daily precipitation in regional climate models over Europe. *Theoretical and Applied Climatology*, *99*, 187–192.

Piani, C., Weedon, G. P., Best, M., Gomes, S. M., Viterbo, P., Hagemann, S., & Haerter, J. O. (2010). Statistical bias correction of global simulated daily precipitation and temperature for the application of hydrological models. *Journal of Hydrology*, *395*, 199–215.

Putri, J. K., & Suhadi. (2024). Analisis temperatur ekstrem dan penyebabnya di Indonesia. *Journal Online of Physics*, *10*(1), 27–30.

Robock, A. (2000). Volcanic eruptions and climate. *Reviews of Geophysics*, *38*(2), 191–219.

Salwati, Handoko, & Irsal Las3), dan H. R. (2013). Model Simulasi Perkembangan, Pertumbuhan Dan Neraca Air Tanaman Kentang Pada Dataran Tinggi Di Indonesia. *Informatika Pertanian*, *22*(1), 53.

Seferian, R. (2023). *CNRM-CERFACS CNRM-ESM2-1 model output prepared for CMIP6 CMIP*. World Data Center for Climate (WDCC) at DKRZ. https://www.wdc-climate.de/ui/entry?acronym=C6_4342685

Silvy, Y., Frölicher, T. L., Terhaar, J., Joos, F., Burger, F. A., Lacroix, F., Allen, M., Bernardello, R., Bopp, L., Brovkin, V., Buzan, J. R., Cadule, P., Dix, M., Dunne, J., Friedlingstein, P., Georgievski, G., Hajima, T., Jenkins, S., Kawamiya, M., … Ziehn, T.

(2024). AERA-MIP: Emission pathways, remaining budgets and carbon cycle dynamics compatible with 1.5 °C and 2 °C global warming stabilization. *Earth System Dynamics*, *15*, 1591–1628.

Staunton-Sykes, J., Aubry, T. J., Shin, Y. M., Weber, J., Marshall, L. R., Luke Abraham, N., Archibald, A., & Schmidt, A. (2021). Co-emission of volcanic sulfur and halogens amplifies volcanic effective radiative forcing. *Atmospheric Chemistry and Physics*, *21*(11), 9009–9029.

Supari, Tangang, F., Juneng, L., & Aldrian, E. (2016). Observed changes in extreme temperature and precipitation over Indonesia. *International Journal of Climatology*, *37*(4), 1979–1997.

Wieners, C. E., Hofbauer, B. P., de Vries, I. E., Honegger, M., Visioni, D., Russchenberg, H. W. J., & Felgenhauer, T. (2023). Solar radiation modification is risky, but so is rejecting it: a call for balanced research. *Oxford Open Climate Change*, *3*(1), 1–4.